Acrylic Polymer–Silk Fibroin Blend Fibers

YUYU SUN,[1] ZHENGZHONG SHAO,[1] MINGHUA MA,[2] PING HU,[1,*] YUSHUN LIU,[1] TONGYIN YU[1]

[1] Department of Macromolecular Science, Fudan University, Shanghai, 200433 People's Republic of China

[2] Department of Chemistry, Fudan University, Shanghai, 200433 People's Republic of China

Received 22 July 1996; accepted 5 December 1996

ABSTRACT: Blends of acrylic polymer (containing acrylonitrile 91.7%, methyl acrylate 7%, and sodium methyl propenyl sulfonate 1.3% [wt %], denoted as PAC) with silk fibroin (SF) were studied in the form of drawn fibers with varied compositions. The strength, elongation, and specific work of rupture of the blend fibers decrease with increase of the SF content, whereas the modulus has a slight increase up to 20% (wt) SF and then decreases. With the addition of up to 30% (wt %) SF in the PAC matrix, the moisture absorption increases from 2.06 to 6.2% in comparison with the PAC. Scanning electron microscopy studies show that the blend fibers have a sheath–core structure, with SF mainly in the sheath and PAC in the core. FTIR, ATR, and X-ray diffraction results of the blend fibers are also presented. © 1997 John Wiley & Sons, Inc. J Appl Polym Sci **65:** 959–966, 1997

Key words: silk fibroin; PAC; blend fibers; sheath–core structure

INTRODUCTION

From the textile point of view, almost every commercial available fiber possesses some outstanding characteristics but suffers from some inferior performance. So, many attempts have been made to improve their properties. Among the traditional modification means, blend fibers, which refer to the polymer–polymer blends comprising the individual filament, are the best choice when it is necessary that each fiber has the desired characteristics.[1]

Bombyx mori silk fibroin (SF) has been used as a textile material for thousands of years for its excellent luster, tensile, handle, and moisture absorption. However, it has some shortcomings such as photoyellowing, wrinkle recovery, and rub resistance. Although some studies have been made to improve its properties by graft copolymerization,[2–4] only a few studies in the literature using the method of blending can be found.

Polyacrylonitrile (PAN) and its copolymers (PAC) fibers are widely used as textile and reinforcement fibers as well as the precursor for carbon fibers because of their cheap price and antibacteria and excellent antiphoto oxidization characteristics. However, PAN and PAC fibers, showing low moisture absorption and the collection of static electricity, should be improved and have attracted considerable academic and practical interest.[5–8]

It was thought that PAN–SF or PAC–SF blend fibers would combine the merits of the two fibers and enlarge the range of their applications. Some authors[6a] presented the investigation on PAN–SF blend fibers extruded from aqueous $ZnCl_2$ solutions. Although PAC fibers take a very important role in the acrylic fiber industry, there are only a few studies in the literature on PAC–SF blend systems except for some patents.[6b] The main purpose of this article was to study the morphological and mechanical properties of PAC–SF

Correspondence to: T. Yu.

* *Present address:* 6218 Burke Laboratory, Dartmouth College, Hanover, NH 0375.

Contract grant sponsor: National Science Foundation of China and Target Basic Research.

Table I Maximum Draw Ratios of the Blend Fibers

Blends	PAC	95/5	90/10	80/20	70/30
Maximum draw ratios	9.5	8	6.5	5.2	4.3

blend fibers as a function of the blend ratio. The PAC-rich samples are of special interest.

EXPERIMENTAL

Preparation of PAC–SF Blend Fibers

PAC was kindly supplied by the Jinshan Acrylic Fiber Factory. Pyrolytic chromatography results show that it was made up of acrylonitrile (91.7%), methyl acrylate (7%), and sodium methyl propenyl sulfonate (1.3%), and its molecular weight is 50,000–60,000.

Degummed silk fibroin from waste *Bombyx mori* silk fiber and PAC were each dissolved in 52% (wt) aqueous NaSCN solutions. The blend solutions were made up with water, each having a total polymer concentration of 12% by weight and relative polymer compositions, expressed as PAC/SF weight ratios, of 90/10, 80/20, 70/30, etc. After that, the blend solutions were extruded from a 30 hole (0.08 mm diameter) die into a 10% NaSCN aqueous coagulation bath at 0–5°C to form the fibers. The as-spun fibers were washed and drawn in boiling water, than dried at 120°C for 30 min.

Measurements

Tensile tests were carried out on an Instron machine Model 1121. All tests were performed on single filaments using a gauge length of 50 mm and crosshead speed of 20 mm/min. The average of 50 readings was presented for each sample.

The moisture absorptions of the blend fibers were calculated from increase in the weight of the dried original fibers (dried at 50°C in a vacuum for 1 week) after being conditioned at 20°C and 65% RH for 2 weeks as follows:

$$\text{moisture absorption (\%)} = (W_2 - W_1)/W_1 \times 100 \quad (1)$$

where W_1 and W_2 denote the weights of the original and the conditioned fibers, respectively.

A JSM-T20 scanning microscope instrument (JEOL) was used to study the morphological structure of the blend fibers. For study of the fracture surfaces, the samples were fractured in liquid nitrogen, whereas for other samples, which were used to show the SF component in the blend fibers, the samples were partially immersed into hot DMF at 60°C for some time to dissolve out the

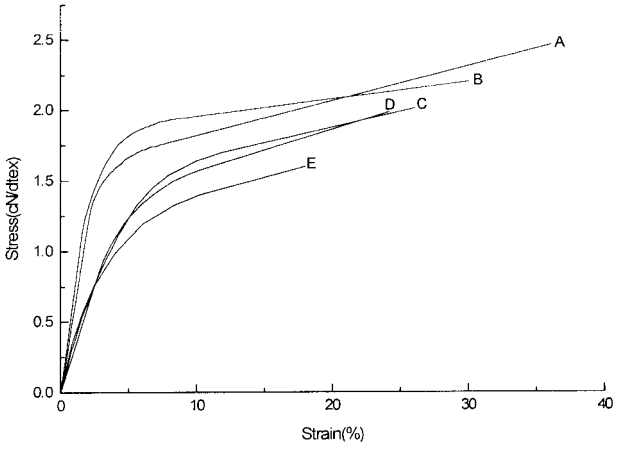

Figure 1 Stress–strain curves of the blend fibers containing (A) 0, (B) 5, (C) 10, (D) 20, and (E) 30 wt % SF.

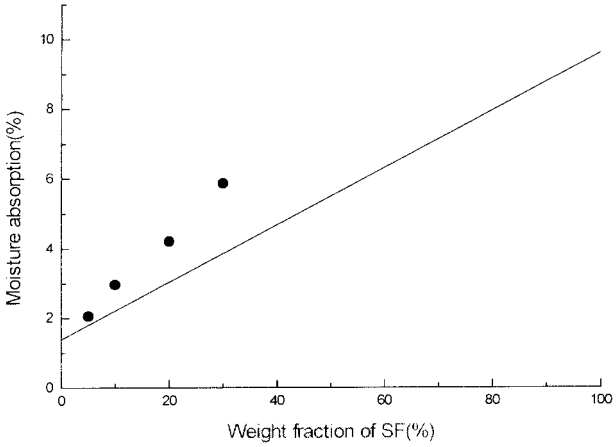

Figure 2 The moisture absorption of the blend fibers as a function of SF content: Straight line: calculated from eq. 2; solid circles: experimental data.

Table II Mechanical Properties of As-spun PAC–SF Blend Fibers

Sample PAC–SF	Strength (cN/dtex)	Initial Modulus (cN/dtex)	Elongation (%)	Specific Work of Rupture (cN/dtex)
100/0	2.46	36.8	36	0.701
95/5	2.20	42.3	30	0.574
90/10	2.00	44.5	26	0.404
80/20	1.98	48.4	24	0.358
70/30	1.60	30	18	0.218

PAC. The resultant fibers were then washed and dried. All the samples were then coated with gold under a vacuum.

FTIR spectra were recorded on a MANGNA IR-550 (Nicolet) spectrometer by the method of transmission. The fibers were crushed in liquid nitrogen and then examined in KBr discs. The samples were made thin enough so to obey the Beer–Lambert law.

ATR spectra were recorded on a Bio-Rad Digilab FTS-20 ATR spectrometer. Fibers were wound around a 5 mm-thick KRS-5 prism. In this study, the incident angle is 62° and the examined thickness was estimated to be several microns. X-ray diffraction measurements of the fibers were performed with a D-MAX/II-A diffractometer, using CuKα radiation (λ = 1.54 Å) in the 2θ range of 5–35°.

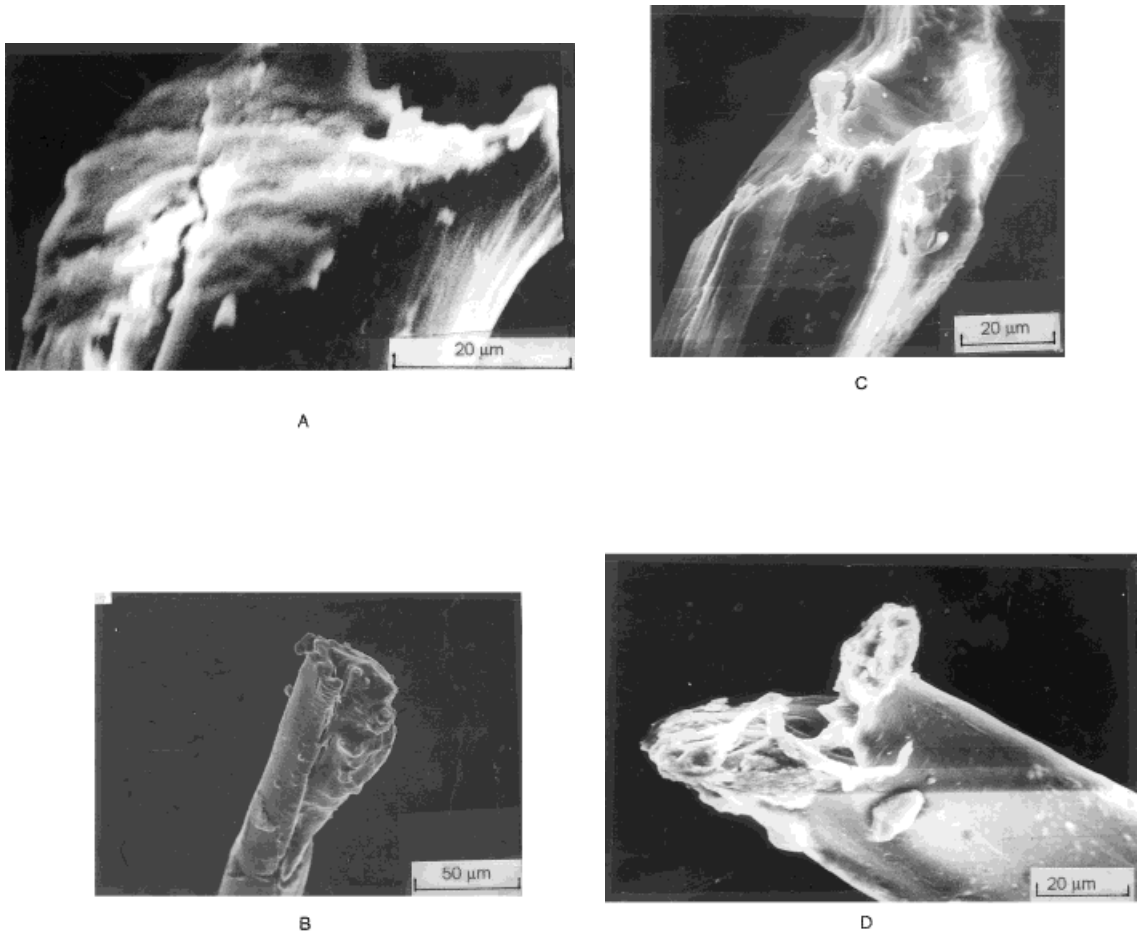

Figure 3 SEM photomicrographs of the fracture surfaces of the blend fibers containing (A) 0, (B) 10, (C) 20, and (D) 30 wt % SF.

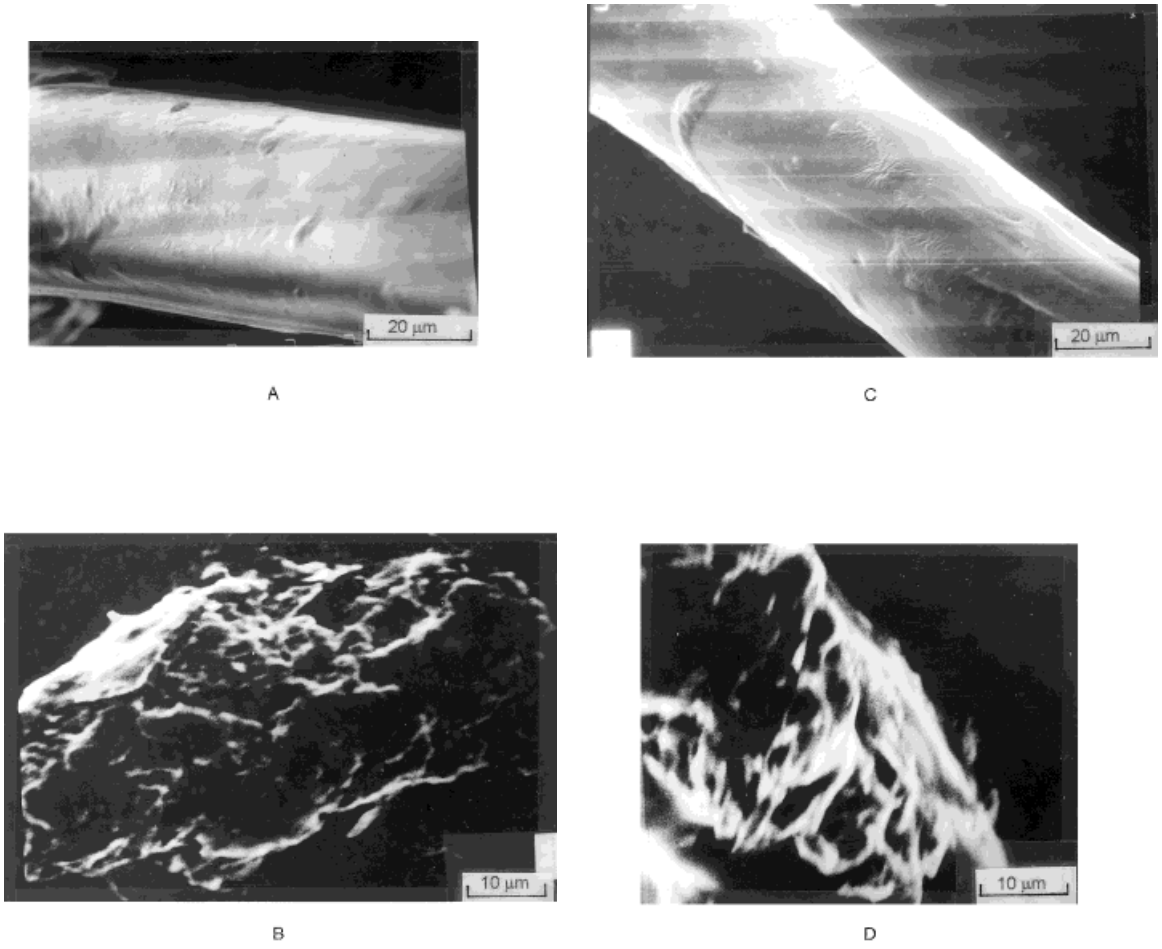

Figure 4 SEM photomicrographs of the blend fibers: (A) 80/20, before etched in DMF, longitudinal section; (B) 80/20, after etched in DMF, longitudinal section; (C) 70/30, before etched in DMF, longitudinal section; (D) 70/30, after etched in DMF, longitudinal section; (E) 70/30, before etched, cross section; (F) 70/30, after etched in DMF, cross section; (G) 70/30, after etched in aqueous LiBr solution (9.5*M*), cross section.

RESULTS AND DISCUSSION

Drawing

Table I shows the relation between the maximum draw ratio and the composition of the blends. One can see that with increase of the SF content the maximum draw ratio decreases. This may be attributed to (a) the poor adhesion between SF and PAC, because if a blend is roughly dispersed and the boundary between the components is weak, the maximum draw ratio must be restricted by breaking at the boundary region, as shown by the SEM results, and (b) the molecular weight of SF used in this study was probably decreased by the dissolution treatment with NaSCN. Because in this study PAC is the major component of the blend fibers, all the samples were drawn to the maximum draw ratios.

Mechanical Properties

Figure 1 shows the stress–strain curves of the blend fibers; data are given in Table II. It can be seen that with increase of the SF component the strength, elongation, and specific work of rupture of the blend fibers decrease. Although there may be numerous possible reasons for this phenomenon, we believe that two of them stand out prominently. First, as shown in the XRD study, no evidence for the existence of crystalline SF was found, and the fraction of the amorphous SF component would influence the properties of the blend

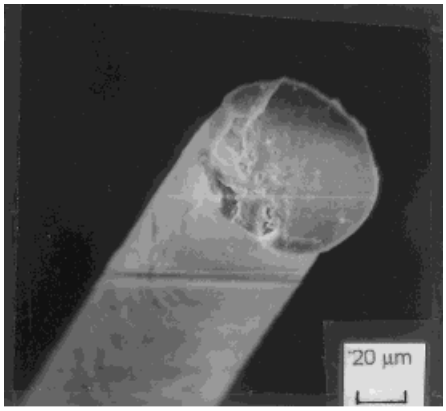

E

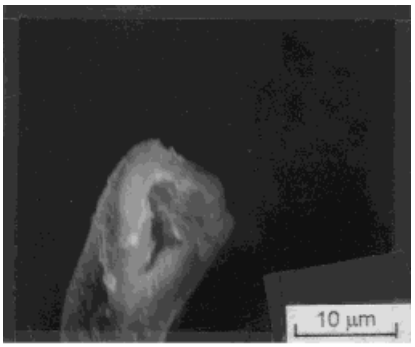

F

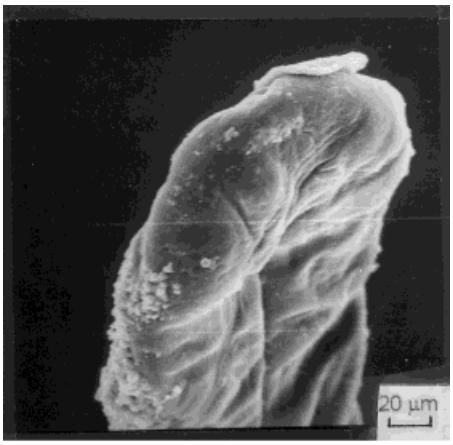

G

Figure 4 (*Continued from the previous page*)

fibers. Second, as demonstrated in IR spectroscopy, the specific interaction between PAC and SF must be small, so the weak boundary must influence the strength, elongation, and specific work of rupture of the blend fibers, which is, in essence, consistent with the SEM photomicrographic study. In a lower weight percentage of SF content, the initial modulus of the blend fibers increases with increase of the SF component, whereas at a higher percent of the SF content, say, higher than 30%, the initial modulus decreases.

It should be pointed out that there is no reason to believe that spinning conditions selected here are the optimum conditions. Therefore, the mechanical properties of the blend filaments, obtained in present study, may be improved by choosing more suitable spinning conditions, which will be the main subject of our further study. However, it can be seen that in lower SF content (up to 20%) the mechanical properties of the blend fibers have already characterized them as usable fibers.

Moisture Absorption

The moisture absorption of the blend fibers is plotted in Figure 2 as a function of the weight fraction of SF in order to elucidate the composition dependence of the blends. The 100% SF samples were represented by the original degummed silk fibroin from wasted silk fiber. The line in Figure 2 is calculated from

$$A_b = \omega_p A_p + \omega_s A_s \qquad (2)$$

where A_b, A_p, and A_s denote the moisture absorption of the blends, PAC, and SF, respectively, whereas ω_p and ω_s represent the weight fraction of PAC and SF in the blends, respectively. The scattered circles in Figure 2 are the data obtained in the experiment. Figure 2 shows that the amount of moisture absorption increases with the amount of SF present, but not linearly. The deviation from linearity suggests that: (i) the crystallinity of SF in the blends must be low, in comparison to pure SF, which is proved by the result obtained by the X-ray measurement, and/or (ii) the boundary in the blends may serve an important role in the moisture absorption of the blend fibers.

SEM Photomicrographs

Figure 3 shows the fracture surface of the blend fibers fractured in liquid nitrogen. The fracture surface of PAC [Fig. 3(A)] shows some extent of the ductile fracture as well as the brittle fracture mode, and there is a small number of cracks away from the fracture site. The fracture surfaces of the

blends show other kinds of modes: When the SF content is low (less than 20 wt %), there are heavy cracks between the sheath and the core of the fibers [Fig. 3(B) and (C)], which is thought to indicate that the structure of the sheath and the core of the blend fibers are different and the adhesion between them is weak. In a higher SF content (30 wt %), gross defects as long as fibrils were observed in the immediate region of the fracture area [Fig. 3(D)], which must be caused by phase separation and/or poor adhesion.

The "sheath–core" idea is further strengthened by the photomicrographs in Figure 4. Figure 4 shows the longitudinal sections of the 80/20 and 70/30 blend fibers and the cross sections of the 70/30 samples before and after being etched in hot DMF. The surfaces of the blend fibers are very smooth as shown in Figure 4(A) and (C). After being etched in hot DMF, most of the PAC component was dissolved, and it can be seen that the SF component is mainly in the sheath of the blend fibers, forming a continuous "skin," whereas in the core, discontinuous SF fibrils can also be observed [see Fig. 4(B), (D), and (F)]. This kind of morphology has been reported by a number of authors in other blend systems, and it is believed that[9,10] this morphology is controlled by the relative rheological characteristics of the two polymers. After all, this morphology has important implications for luster, handle, moisture absorption, and wearing comfort of the blend fibers.

FTIR and ATR Spectra

Figure 5 shows the FTIR and ATR spectra of the blends in the range of 2400–1100 cm^{-1}. The FTIR spectra of the blend fibers (A–C, containing 10, 20, and 30 wt % SF, respectively) show absorption bands at 2243, 1735, and 1454 cm^{-1}, which are attributed to the PAC component in the blends. One can also observe the typical absorption bands of SF at 1629 (amide I), 1530 (amide II), and 1265 (amide III), assigned to the silk II form,[11] and the bands at 1658 (amide I) and 1235 (amide III), attributed to random coil[11] or silk I form.[12] Asakura and co-workers[13] even claimed that the distinction between the silk I form and random coil forms from IR spectra is impossible.

One can obtain some information about the surface structure of the blend fibers by ATR spectra as shown in Figure 5 (D–F, containing 10, 20, and 30 wt % SF, respectively); the examined thickness was estimated to be several microns. The ATR spectra also show the absorption bands mentioned above, but the band shapes of the SF component attributed to amide I, amide II, and amide III are different, and as to amide III, only the 1265 cm^{-1} band can be detected, instead of the 1235 and 1265 cm^{-1} in the FTIR spectra. This result may indicate that not only the composition in the sheath and core of the blend fibers (as seen in the SEM study) is different but also the configuration of the SF component in the sheath and core. Careful study can also obtain a quantitative estimate of the composition of the fiber surface according to Sibila's method.[14] However, in this study, the composition of silk I and silk II forms of SF in the blends as well as the absorption ratio of these two forms are difficult to get, and we do not think we can get the quantitative estimate at the present time.

It should be pointed out that in a separate study we found that the carbonyl group of PAC can form hydrogen bonds with SF, as determined by an FTIR study, whose intensity depends upon the methyl acrylate content in PAC and the composition of the blends, and when PAC was made up of 85% acrylonitrile and 15% methyl acrylate (mol %), the intensity of the hydrogen bands, which were centered at 1703 cm^{-1}, is the strongest, as shown in Figure 6 (details of this study will be presented elsewhere). But in the present study, we did not observe any trace of hydrogen bands between PAC and SF, which must be caused by the unsuitable PAC composition. These findings suggest that the specific interaction between PAC and SF is small, implying that the two polymers are incompatible.

X-ray Diffraction

Figure 7 shows the X-ray diffraction patterns of PAC and the blend fibers. PAC [Fig. 7(A)] shows on the equator a rather strong and relatively sharp reflection with a Bragg spacing $d = 5.24$ Å presented, in agreement with the literature data.[15,16] SF [see Fig. 7(E); this sample was represented by the original degummed silk fibroin from wasted silk fiber] shows a reflection at $d = 4.5$ and $d = 4.69$ Å, assigned to the silk I and silk II forms, respectively.[15] Upon blending, the 4.5 and 4.69 Å reflections disappear, suggesting that the crystallinity of SF in the blend fibers is rather low, which may have some favorable influence on the moisture absorption of the blends. On

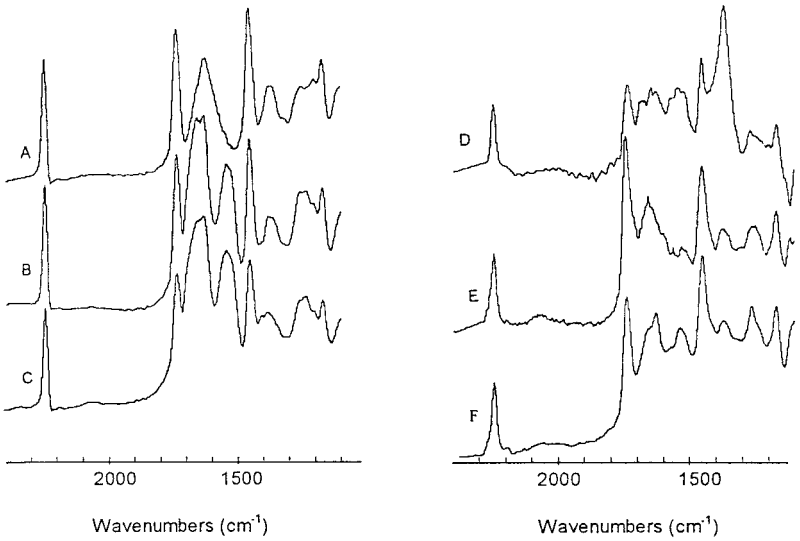

Figure 5 IR spectra of the blend fibers: (A) 90/10, FTIR; (B) 80/20, FTIR; (C) 70/30, FTIR; (D) 90/10, ATR; (E) 80/20, ATR; (F) 70/30, ATR.

the other hand, all the blends [Fig. 7(B)–(D)] under study show the typical reflection of PAC, and with increase of the SF content, the reflection slightly shifts to smaller angles. This result implies that the SF component has no noticeable influence on the "crystal structure"[17] or the "ordered domains"[18] of PAC in the blend fibers.

CONCLUSION

The results of the present study can be summarized as follows:

1. With increase of the SF content, the maximum draw ratio, strength, elongation, and specific work of rupture of the blend fibers decrease, whereas initial modulus increases up to 20% SF (wt) and then decreases with increase of the SF content.

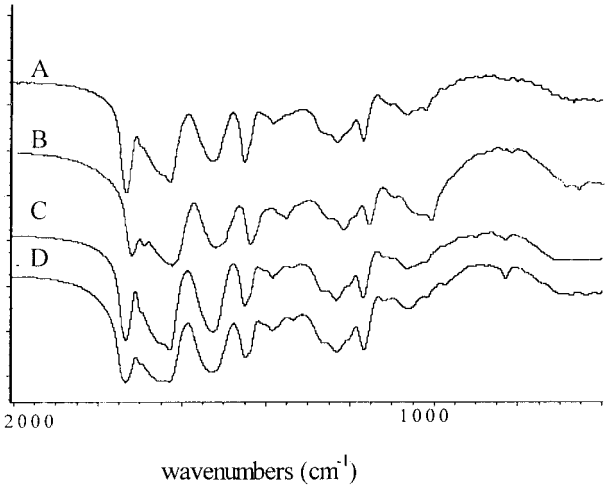

Figure 6 FTIR spectra of poly(AN-*co*-MA)–SF 50/50 (wt %) blends. Poly(AN-*co*-MA) containing (A) 9, (B) 15, (C) 23, and (D) 36 mol % methyl acrylate.

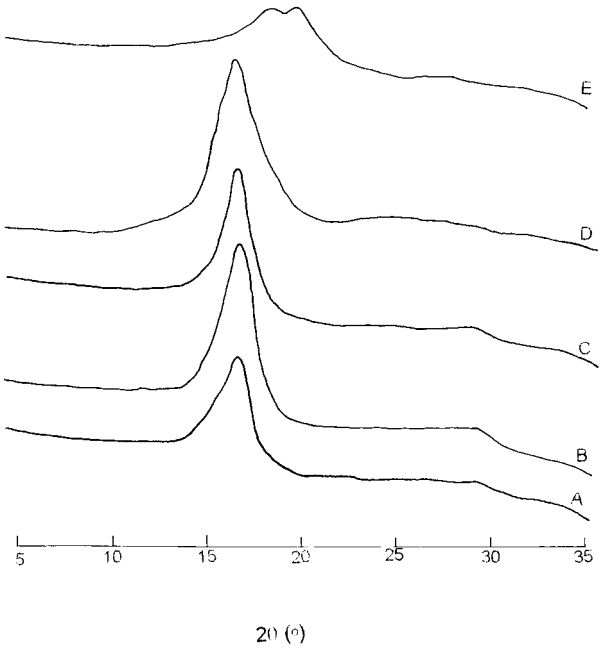

Figure 7 X-ray diffraction patterns of the blend fibers containing (A) 0, (B) 10, (C) 20, (D) 30, and (E) 100 wt % SF.

2. The moisture absorption of the blend fibers increases with increase of the SF content, but not linearly.
3. The blend fibers have a sheath–core structure, and SF is mainly in the sheath of the blend fibers, whereas in the core, discontinuous SF fibrils can also be observed. Also, the configuration of the SF component in the sheath and in the core are different.
4. The "crystal structure" or the "ordered domains" of PAC in the blend fiber are relatively unchanged upon blending with SF. No evidence for the existence of crystalline SF was found in our present study.

REFERENCES

1. L. Rebenfeld, *Textile Research Institute, Encyclopedia of Polymer Science and Engineering,* 2nd ed., Wiley-Interscience, New York, 1985.
2. M. Tsukada, *J. Appl. Polym. Sci.,* **35,** 2133 (1988).
3. M. Tsukada, M. Nagura, H. Ishikawa, and H. Shiozaki, *J. Appl. Polym. Sci.,* **49,** 593 (1993).
4. J. Liu and T. Yu, *Fudan Xue Bao (Ziran Kexue Ban)* (in Chinese), **33,** 371 (1994).
5. D. M. Cates and H. J. White, Jr., *J. Polym. Sci.,* **20,** 155 (1956).
6. (a) D. M. Cates and H. J. White, Jr., *J. Polym. Sci.,* **21,** 125 (1956); (b) P.R. China Pat. CN 1,107,906A.
7. P. Lennox-Keer, *Tex. Inst. Ind.,* **19,** 83 (1983).
8. J. Qin, *J. Appl. Polym. Sci.,* **44,** 1095 (1992).
9. D. R. Paul and S. Newman, *Polymer Blends,* Academic Press, New York, San Francisco, London, 1978.
10. W. Xiao, *J. Appl. Polym. Sci.,* **52,** 1023 (1994).
11. J. Magoshi, M. Mizuide, Y. Magoshi, K. Takahashi, M. Kubo, and S. Nakamura, *J. Polym. Sci. Polym. Phys. Ed.,* **17,** 515 (1979).
12. T. Hayakawa, K. Kondo, S. Yamamoto, and J. Noguchi, *J. Kobunshi Kagaku,* **27,** 300 (1970).
13. T. Asakura, A. Kuzuhara, R. Tabeta, and H. Saito, *Macromolecules,* **18,** 1841 (1985).
14. J. P. Sibila, *J. Appl. Polym. Sci.,* **17,** 2911 (1973).
15. R. Hosemann and P. H. Lindenmeyer, *J. Appl. Phys.,* **34,** 42 (1963).
16. J. J. Klement and P. H. Geil, *J. Polym. Sci. Polym. Phys. Ed.,* **6,** 1381 (1968).
17. G. J. Hinrichsen, *J. Polym. Sci. C,* **38,** 303 (1972).
18. C. N. Tyson, *Nature, Phys. Sci.,* **233,** 118 (1971).